The presented research comes from Professor Tao Chen's group at Ningbo Institute of Materials Technology and Engineering, Chinese Academy of Sciences, China.

Dynamic metal–ligand coordination enables a hydrogel with rewritable dual-mode pattern display

This study presents a hydrogel-based optical platform integrating dynamic metal–ligand coordination for rewritable dual-mode information display. The system features a robust poly(dodecylglyceryl itaconate) (pDGI) lamellar structure and flexible poly(acrylamide)/poly(acrylic acid) (PAAm/PAAc) networks with embedded fluorescent carbon dots (CDs). Metal ions like Al^{3+} induce color changes, while EDTA restores original colors, enabling erasable information display. This research advances materials for enhancing security in rewritable information systems.

As featured in:

See Xiaoxia Le, Tao Chen *et al.*, *Mater. Horiz.*, 2024, **11**, 5244.

ROYAL SOCIETY OF CHEMISTRY

rsc.li/materials-horizons

Registered charity number: 207890

Materials Horizons

ROYAL SOCIETY OF CHEMISTRY

COMMUNICATION

View Article Online
View Journal | View Issue

Cite this: *Mater. Horiz.*, 2024, 11, 5244

Received 30th July 2024,
Accepted 5th September 2024

DOI: 10.1039/d4mh00996g

rsc.li/materials-horizons

Dynamic metal–ligand coordination enables a hydrogel with rewritable dual-mode pattern display†

Hui Shang,‡[ab] Yu Sun,‡[ab] Xiaoxia Le,*[ab] Ying Shen[ab] and Tao Chen*[abc]

The realization of dual-mode information display in the same material is of great significance to the expansion of information capacity and the improvement of information security. However, the existing systems lose the ability to re-encode information once they are constructed. Here, dynamic metal–ligand coordination is introduced into a novel hydrogel-based optical platform that allows rewritable dual-mode information display. The hydrogel system consists of a hard lamellar structure of poly(dodecylglyceryl itaconate) (pDGI) and soft double networks of poly(acrylamide)/poly(acrylic acid) (PAAm/PAAc) containing fluorescent carbon dots (CDs). As the carboxylic acid groups can coordinate with metal ions such as Al^{3+}, the layer spacing of the lamellar structure is reduced while CDs aggregate, leading to the blue shift of the structural color and the red shift of the fluorescent color. Additionally, the metal chelating agent, ethylenediaminetetraacetic acid (EDTA), is able to strip away Al^{3+} ions and restore the two colors, realizing an erasable dual-mode information display. This study opens up a path for the development of new materials and technologies for rewritable dual-mode information protection.

New concepts

With technological advancements, there is an increasing demand for materials capable of securely storing and dynamically displaying information in multiple modes, including the ability to modify content post-deployment. This paper introduces a novel dynamic dual-mode optical hydrogel material utilizing dynamic metal ion coordination, combining a rigid pDGI multilayer structure with flexible PAAm/PAAc polymeric networks incorporating solvatochromic fluorescent CDs. Adding metal ions like Al^{3+} tightens the pDGI multilayer structure and promotes CD aggregation, enabling a shift between structural color and fluorescence. Post-coordination, EDTA interacts with Al^{3+} ions within the hydrogel, removing them to restore the material's original color, facilitating information erasure and modification. This study introduces an innovative optical display platform that can read information under both visible and ultraviolet light. It also supports loading, erasing, and reloading of the programmed patterns. This system pioneers dual-mode reading and rewritable optical technology, opening new avenues for research and practical applications.

Introduction

Establishing robust information protection platforms is crucial in combating the growing issues of false information and information leaks *etc.*[1–5] These platforms have evolved significantly from static, single-mode information displays to dynamic, multi-channel information decryption systems, which have been driven by advancements in both new materials and techniques.[6–9] In particular, dual-mode optical information display refers to a technology that combines two distinct display modes within a single system, offering enhanced versatility and functionality.[10–12]

One typical dual-mode optical display involves the integration of reflective and emissive display technologies, such as fluorescence and structural color.[13–16] For example, Yu's group[17] developed a "two-color" photonic ink with adjustable reflection color and stable fluorescence, which is controlled by the liquid crystal's spiral superstructure and the molecular structure of the fluorescent material. This dual-label system exhibits distinct patterns in reflection and fluorescence modes. Yang's team[18] proposed a polymer-stabilized cholesteric liquid crystal system with highly temperature-sensitive structural color, photosensitive pigment, and fluorescence color. The structural color changes from red to blue and the fluorescent color varies from blue to red by temperature transition, realizing the transmission of encrypted information with high security. These elegant attempts prove that the dual optical mode of structural color and fluorescent color is

[a] *Key Laboratory of Advanced Marine Materials, Ningbo Institute of Materials Technology and Engineering, Chinese Academy of Sciences, Ningbo 315201, China. E-mail: lexiaoxia@nimte.ac.cn, tao.chen@nimte.ac.cn*
[b] *School of Chemical Sciences, University of Chinese Academy of Sciences, 19A Yuquan Road, Beijing 100049, China*
[c] *College of Material Chemistry and Chemical Engineering Key Laboratory of Organosilicon Chemistry and Material Technology Ministry of Education Hangzhou Normal University Hangzhou, 311121, China*

† Electronic supplementary information (ESI) available. See DOI: https://doi.org/10.1039/d4mh00996g

‡ Hui Shang and Yu Sun contributed equally to this work.

feasible in improving visibility, dynamic content display, and versatility.

Owing to the dynamic and adaptive nature, stimuli-responsive gels[19,20] can change their properties such as color, transparency, or shape in response to a specific stimulus like temperature, pH, light, electric fields, *etc.*, hiding information under normal circumstances and display information under certain stimuli.[21–26] Previously, a dual-mode hydrogel with structural and fluorescent colors was reported for the first time by our group.[11] By changing the layer spacing of the lamellar structure to adjust the structural color and changing the type of coordination lanthanide ions to regulate fluorescence color, this kind of soft material can be used for multistage information encryption. However, once the hydrogels have been fabricated, the corresponding two colors are determined.

Herein, a hydrogel with reversible structural and fluorescent color changes was constructed for rewritable dual-mode patterns *via* the two-step interpenetrating technique. Monomers including dodecylglyceryl itaconate (DGI) and acrylamide (AAm) were firstly photopolymerized to form a rigid lamellar structure and soft hydrogel network. Furthermore, acrylic acid (AAc) bonding CDs penetrated into the PAAm hydrogel network and polymerized to form the second network (Scheme 1A). Metal ions such as Al^{3+} ions could coordinate with carboxylic acid groups, leading to the variation of the structural color ascribed to the change of the lamellar layer spacing as well as the variation of the fluorescent color caused by the aggregation states of CDs (Scheme 1B). Both the structural color and fluorescent color of the hydrogel could be adjusted on-demand by changing the concentration of Al^{3+} ions, and further erased by adding EDTA. As shown in Scheme 1C, original information "SMART" could be encoded as information (MART) as well as "ART" by selectively treating the corresponding letters with Al^{3+} ions, which can be further erased with EDTA solution. These rewritable dual-mode platforms allowed for real-time updates and modifications of displayed content, fostering interactive user experiences and ensuring timely dissemination of information.

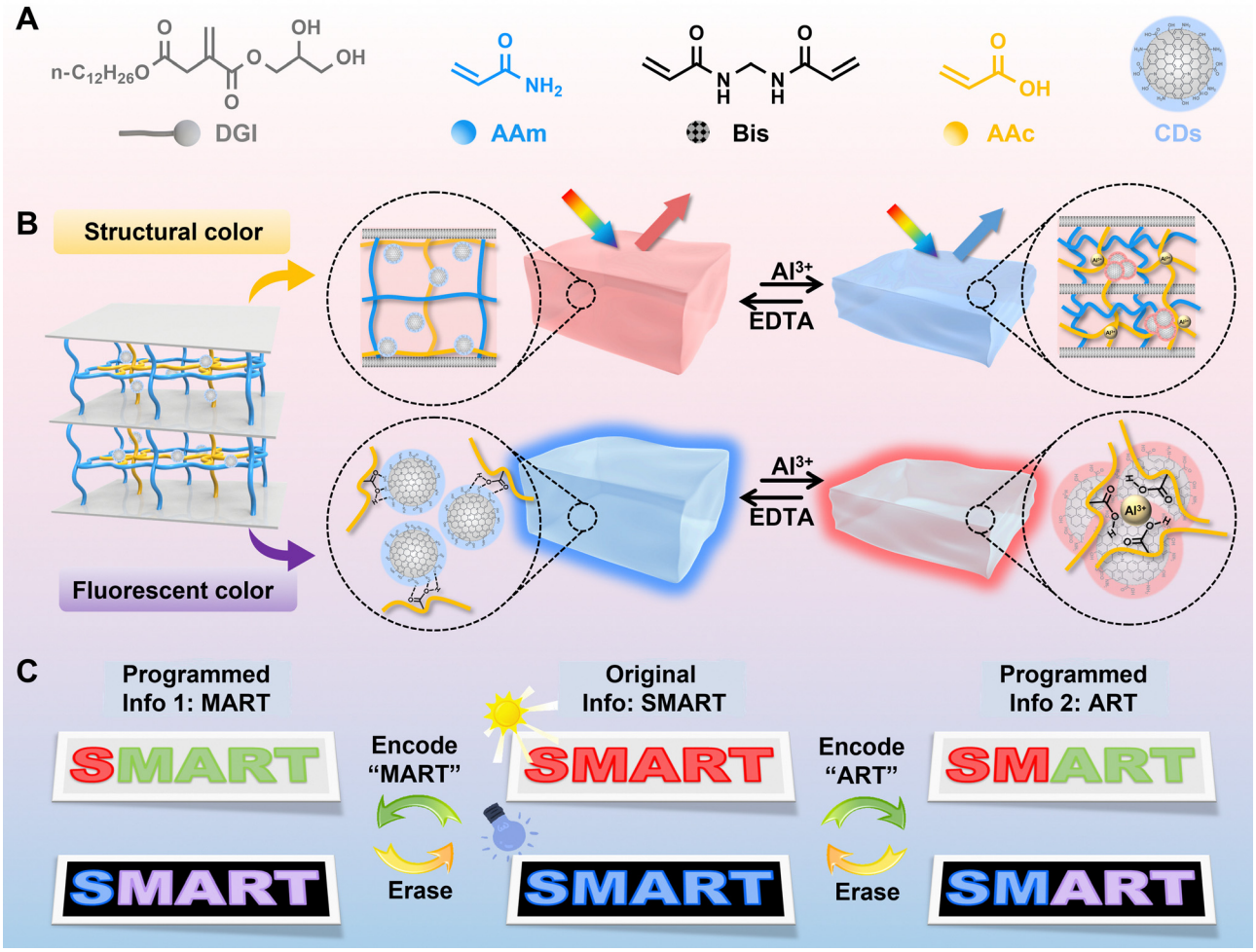

Scheme 1 Dual-mode hydrogel for writable information display. (A) The chemical components used in the construction of the dual-mode hydrogel. (B) Structure diagram of the dual-mode hydrogel, and the coordination of Al^{3+} and the hydrogel towards the variations of structural color and fluorescent color. (C) Schematic of dual-mode hydrogel for rewritable information display from original information (SMART) to programmed information (MART and ART), in which Al^{3+} was used for encoding and EDTA for erasing.

Results and discussion

Synthesis and characterization of double-mode hydrogels (DMHs)

The amphipathic monomer dodecylglyceryl itaconate (DGI) and solvatochromic carbon dots (CDs) (Fig. S1, ESI†) were synthesized according to our previous reports.[11,27] The structure of the synthesized CDs was confirmed by FTIR spectroscopy (Fig. S2, ESI†) and the size of the CDs ranged from 2 to 4 nm, which was characterized by TEM (Fig. S3, ESI†). The former (DGI) is capable of self-assembly into layered structures for achieving structural colors (Fig. S4, ESI†), and the latter can emit different fluorescence in different solvents due to the changes of aggregation states (Fig. S5 and S6, ESI†). Based on the synthesized components, pDGI-PAAm/P(AAc-CDs) hydrogels were fabricated *via* a two-step interpenetrating method, which can further coordinate with Al^{3+} to regulate the structural color as well as the fluorescent color (Fig. 1A). The colors were determined by the concentration of Al^{3+} solution (0 M, 0.05 M, 0.1 M, 0.2 M, 0.4 M, 0.6 M, 0.8 M, 1 M, 1.2 M), and for convenience, the corresponding hydrogels were named DMH_0, $DMH_{0.05}$, $DMH_{0.1}$, $DMH_{0.2}$, $DMH_{0.4}$, $DMH_{0.6}$, $DMH_{0.8}$, $DMH_{1.0}$, and $DMH_{1.2}$.

The introduction of Al^{3+} could coordinate with carboxyl groups on PAAc polymer chains and increase the crosslinking density of the hydrogel network, which can be observed by scanning electron microscopy (SEM). As illustrated in Fig. 1B and C, the initial gel pore size of ~50 μm was reduced to ~10 μm after being treated with Al^{3+} ions, which were uniformly distributed in the hydrogel (Fig. 1D). To verify the coordination between carboxylic acid groups and Al^{3+} ions, ATR-FTIR and Raman were conducted. As shown in Fig. 1E, the hydroxyl peak originating from the carboxyl group at 3415 cm^{-1} disappears and the stretching vibration peak of –C═O– undergoes a blue shift from 1602 cm^{-1} to 1589 cm^{-1} upon coordination with Al^{3+} ions, confirming the interaction. In the meantime, the vibration peak of the C═O bond in acrylic acid (1601.5 cm^{-1}) splits into two distinct peaks, including a blue-shifted peak at 1589.46 cm^{-1} and an uncoordinated peak at 1602.5 cm^{-1} (Fig. 1F), which also proves the coordination between Al^{3+} ions and carboxylic acid groups.

In addition, the mechanical properties of DMHs also dramatically changed after the introduction of Al^{3+} ions. The storage modulus of the hydrogel increased tenfold and the tensile strength rose from 76 kPa to 102 kPa (Fig. S7 and S8, ESI†). One interesting phenomenon worth mentioning was that the structural color and fluorescent color of the DMHs would change after the introduction of Al^{3+} ions, which was also the focus of our follow-up studies. As demonstrated in Fig. 1G,

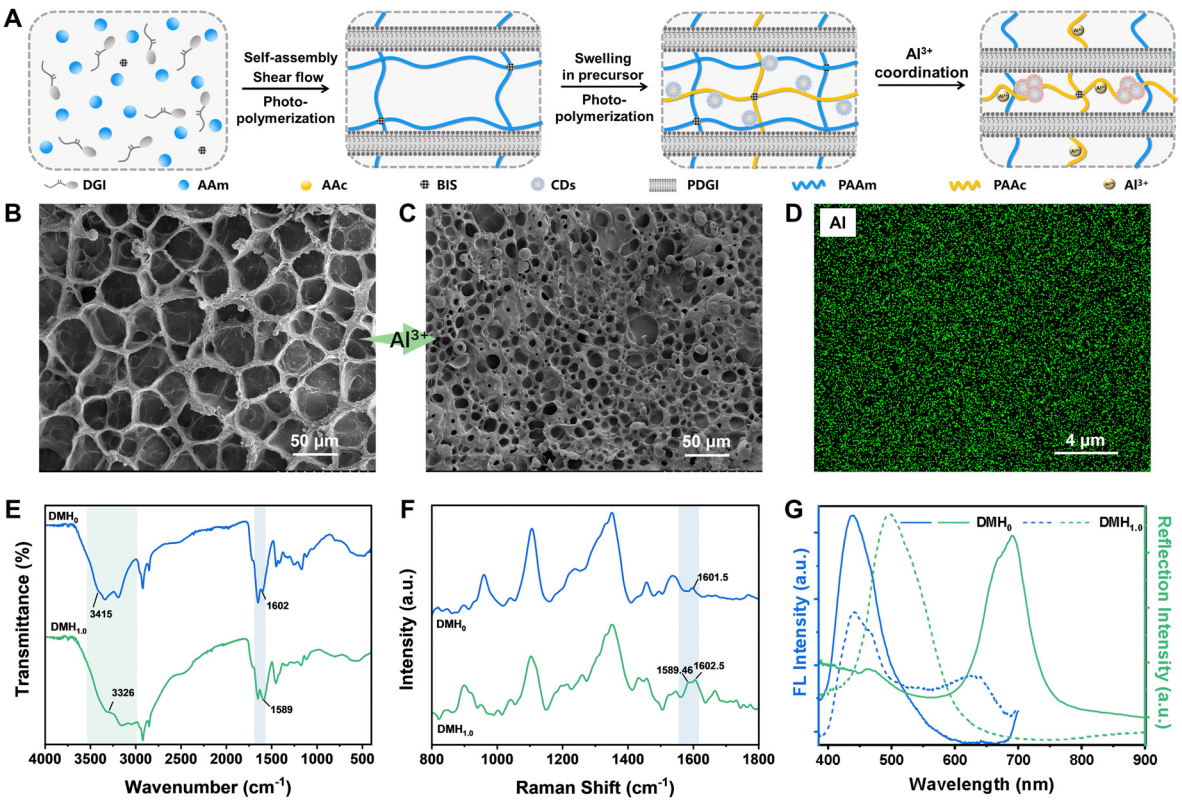

Fig. 1 Preparation and characterization of dual-mode hydrogels with or without Al^{3+} ions. (A) The flow chart of preparing dual-mode hydrogels and the coordination process with Al^{3+} ions. (B) and (C) SEM images of pDGI-PAAm/P(AAc-CDs) hydrogel before and after coordinating with Al^{3+} ions. (D) EDS mapping of Al in pDGI-PAAm/P(AAc-CDs) after being treated with Al^{3+} solution. (E) ATR-FTIR spectra and (F) Raman spectra of pDGI-PAAm/P(AAc-CDs) hydrogel before and after coordinating with Al^{3+}. (G) Fluorescence spectra (λ_{ex} = 365 nm) and reflection spectra of the dual-mode hydrogel before and after coordinating with Al^{3+}.

the structural color varied from purple-red (700 nm) to green (510 nm) and the superimposed fluorescent color changed from blue to pink-red with a reduced blue emission (440 nm) and an enhanced red emission (640 nm) upon Al^{3+} coordination.

Controllable adjusting of the structural colors of DMHs

It is well known that the structural colors arise from the diffraction of light on the periodic nanostructure. Thus, the periodic arrangement of the lamellar structure endows DMHs with bright structural colors. According to Bragg's diffraction law ($2d\sin(\alpha) = n\lambda$), the structural colors of the DMHs were determined by the layer spacing, which can be adjusted by Al^{3+} ions that coordinate carboxylic acid groups on the PAAc polymer chains (Fig. 2A). As illustrated in Fig. S9 (ESI†), the distance of the lamellar was narrowed with the introduction of Al^{3+} ions, resulting in a blue-shift in the structural color.[28–30] During our experiments, we noticed that DMHs treated with Al^{3+} solutions for different times showed different colors (Fig. S10, ESI†), and the color became stable when the processing time was 5 min. Thus, we chose the treatment time of 5 min for the following experiment and demonstrations. As shown in Fig. 2B, the initial DMH was red and gradually changed to yellow and green with the increase of the Al^{3+} concentration. We found that there is no noticeable change in the planar view of the hydrogel before and after treatment with Al^{3+}, but there is significant shrinkage in the vertical direction (Fig. S11, ESI†). Correspondingly, the layer spacing of pDGI reduced from 78 nm to 25 nm, which could be directly confirmed by the SEM images (Fig. 2C). Moreover, small-angle X-ray scattering (SAXS) was further utilized to characterize the decrease of the layer spacing (Fig. S12, ESI†), and the results show that the scattering vector q increases with the increase of the Al^{3+} concentration, which exactly proves this. Additionally, the reflection peaks of DMHs on the reflection spectra had a blue shift of 300 nm and the related CIE chromaticity coordinates also changed as the concentration of the coordination Al^{3+} increases (Fig. 2D and E). More importantly, the Al^{3+} ions could be removed with the action of ion chelating agent EDTA to achieve complete restoration of the structural color, which exhibited excellent repeatability and stability during 10 cycles (Fig. 1F and Fig. S13–S15, ESI†).

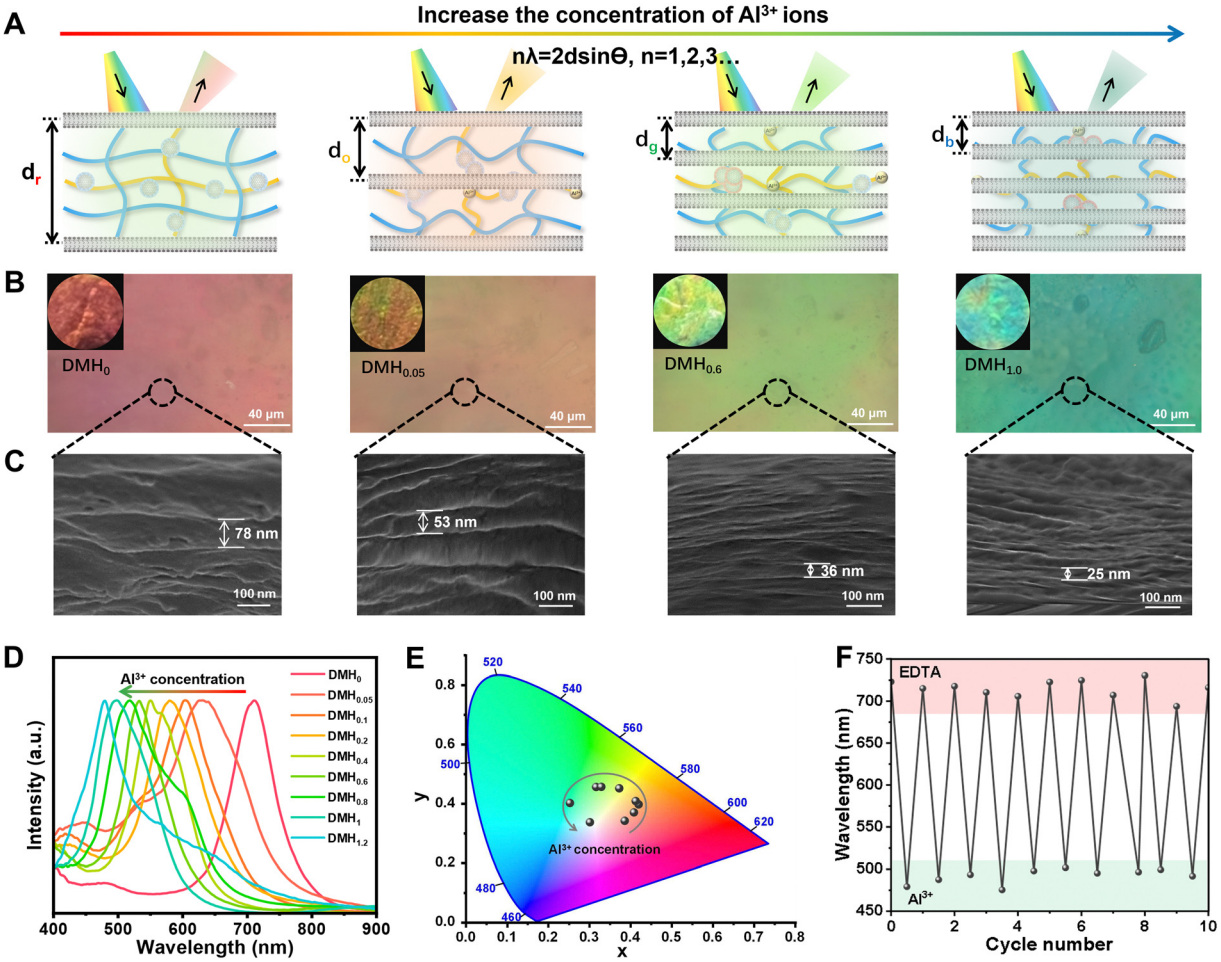

Fig. 2 Structural color of pDGI-PAAm/P(AAc-CDs)-Al^{3+} hydrogels adjusted by the concentration of Al^{3+} ions. (A) Schematic of the structural colors and internal structures of the hydrogels with the increase of Al^{3+} ion concentration. (B) Photographs (inset), reflection optical micrographs and SEM images (C) of DMH_0, $DMH_{0.05}$, $DMH_{0.6}$ and $DMH_{1.0}$. Reflection spectra (D) and CIE chromaticity coordinates (E) of DMH_0, $DMH_{0.05}$, $DMH_{0.1}$, $DMH_{0.2}$, $DMH_{0.4}$, $DMH_{0.6}$, $DMH_{0.8}$, $DMH_{1.0}$, and $DMH_{1.2}$. (F) The changes of the reflection peaks during the process of cyclic Al^{3+} ion coordination and uncoordination.

Controllable regulation of the fluorescent colors of DMHs

In the DMH system, CDs emitting fluorescent color that varied with the aggregation state were synthesized and bonded to the PAAc polymer chains by hydrogen bonding. The introduction of Al^{3+} ions would change the crosslinking density of the hydrogel network, thus we hypothesized that the aggregation state of the CDs changes. To prove this, the luminous centers of the DMHs before and after coordinating with Al^{3+} were characterized. Initially, the luminous center of DMH was mainly concentrated at 420–480 nm (DMH_0), which red-shifted to 500–600 nm ($DMH_{1.0}$) after the introduction of Al^{3+} ions (Fig. 3A and B and Fig. S16, ESI†). It was found that the intensity of the blue emission peak (440 nm) for the dispersed CDs gradually decreased, while the intensity of the red emission peak (640 nm) for the aggregated CDs increased, leading to the fluorescence intensity ratio I_{440nm}/I_{640nm} gradually decreasing from 4.76 to 1.34 and the fluorescence color of DMH changing from blue to pink (Fig. 3C and D). Moreover, the fluorescence lifetime of DMHs showed a gradual weakening trend from 7.54 ns to 3.94 ns (Fig. 3E) and the CIE chromaticity coordinates moved from blue to pink (Fig. 3F) as the concentration of Al^{3+} ions increased. Notably, the DMHs also have good cyclic properties similar to structural colors (Fig. 3G and Fig. S17, ESI†). As demonstrated in Fig. 3H, the Al^{3+} coordination brought the PAAc polymer chains closer together, thereby promoting the aggregation of CDs and resulting in a fluorescence color shift from blue to pink.

Rewritable dual-mode pattern display based on DMHs

As demonstrations of rewritable dual-mode patterns based on DMHs, numbers, patterns and letters were designed. For instance, the "SMART" string (Fig. 4A) could be encoded into different messages such as "MART" and "ART" when treating

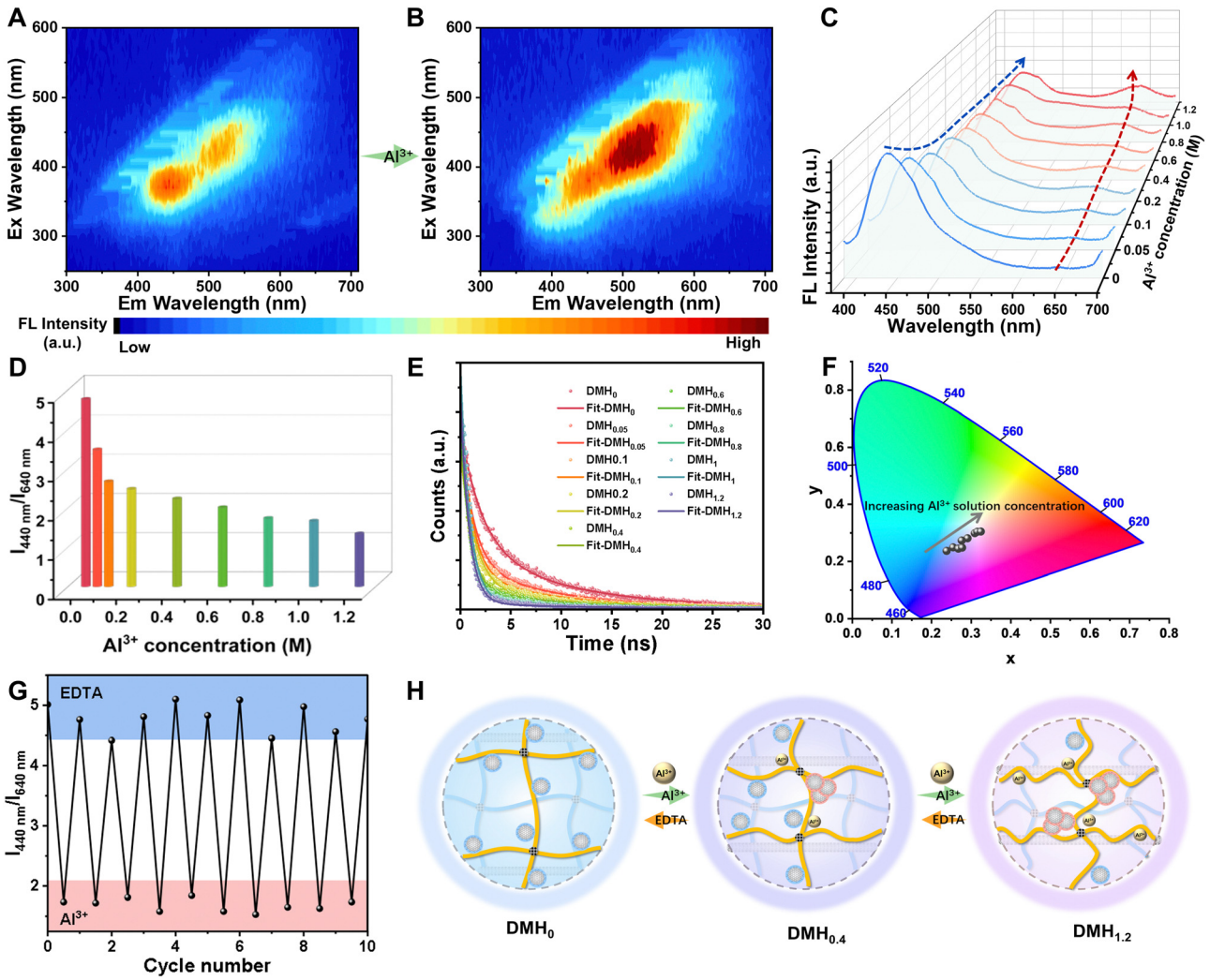

Fig. 3 Fluorescent color of pDGI-PAAm/P(AAc-CDs)-Al^{3+} hydrogels adjusted by the concentration of Al^{3+} ions. (A) and (B) PL mapping spectra of DMHs before and after coordinating with Al^{3+}. (C) Fluorescence spectra (λ_{ex} = 365 nm) of DMHs varying with Al^{3+} ion concentration. (D) The fluorescence intensity ratio I_{440nm}/I_{640nm} varying with Al^{3+} ion concentration. The fluorescence lifetime (E) and CIE chromaticity coordinates (F) of the DMHs (DMH_0, $DMH_{0.05}$, $DMH_{0.1}$, $DMH_{0.2}$, $DMH_{0.4}$, $DMH_{0.6}$, $DMH_{0.8}$, $DMH_{1.0}$, and $DMH_{1.2}$) at 440 nm. (G) The cyclic fluorescent changes of $DMH_{1.0}$ during the process of cyclic Al^{3+} ion coordination and uncoordination. (H) The mechanism schematic of fluorescence color variation.

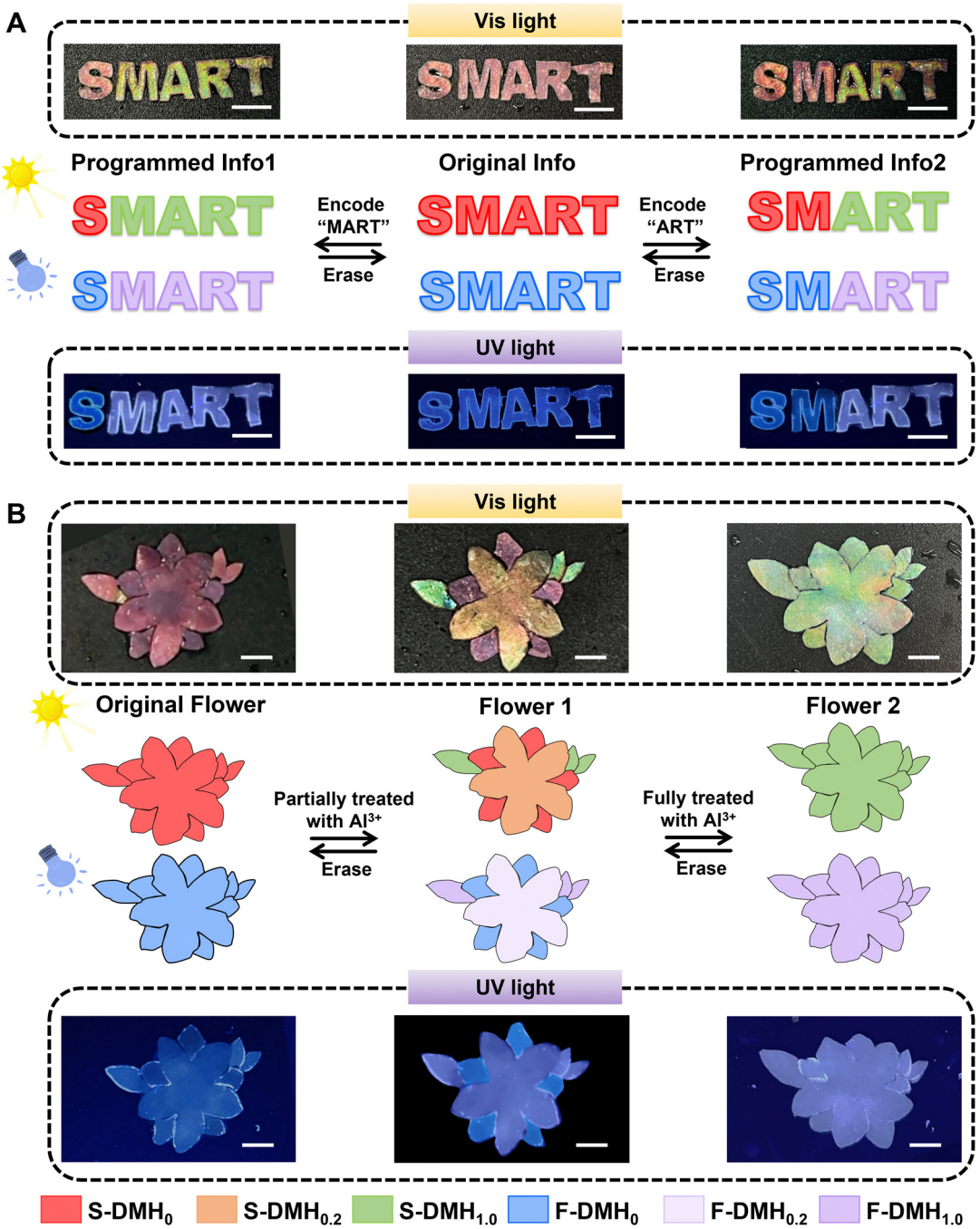

Fig. 4 DMHs for rewritable dual-mode pattern display. (A) A string of letters "SMART" can be encoded into different messages ("MART", "ART") by treating different letters with Al^{3+} ions. (B) A flower that can be transformed into a different color by a designable treatment of aluminum ions with various concentrations.

the corresponding letters with Al^{3+} solution (1.0 M). Since the introduction of Al^{3+} ions could change both the structural color and the fluorescent color, the information would be seen in both visible light and ultraviolet light. Similarly, a red flower (Fig. 4B) changed into a colorful flower when treating different parts with distinct concentrations of Al^{3+} solutions ($DMH_{0.2}$: yellow, $DMH_{1.0}$: green), shifting from blue to blue-purple under UV light. When the whole flower was treated with a highly concentrated Al^{3+} solution (1.0 M), the pattern turned to green. All the above patterns could recover to red (structural color)/blue (fluorescent color) when treated with EDTA solution due to the removal of Al^{3+} ions, achieving a rewritable dual-mode pattern display. Besides, encoded numbers "2024" and "0831" could be presented successively in dual modes, and the fireworks can change colors by processing the related DMHs with Al^{3+} solution and EDTA solution (Fig. S18 and S19, ESI†).

Conclusion

In conclusion, we introduce dynamic metal–ligand coordination into a novel hydrogel-based optical platform, which facilitates rewritable dual-mode information display. The hydrogel system comprises a robust lamellar structure of pDGI and flexible dual networks of PAAm/PAAc embedded with fluorescent CDs. The carboxylic acid groups within the hydrogel can coordinate with metal ions such as Al^{3+}, causing the lamellar structure to contract and CDs to aggregate. This results in a blue shift in structural color and a red shift in fluorescence emission. Furthermore, EDTA is capable of removing Al^{3+} ions, thereby restoring the initial colors and enabling an erasable dual-mode information display. This innovative approach not only demonstrates the feasibility of creating dynamically responsive optical materials but also opens avenues for developing advanced technologies in rewritable dual-mode information systems.

Author contributions

Hui Shang: methodology, data curation, formal analysis, investigation, writing – original draft. Yu Sun: data curation, supervision. Xiaoxia Le: conceptualization, formal analysis, writing – review & editing, supervision. Ying Shen: data curation, supervision. Tao Chen: supervision, conceptualization.

Data availability

The data supporting this article have been included as part of the ESI.†

Conflicts of interest

There are no conflicts to declare.

Acknowledgements

The authors thanked Prof. Patrick Theato from the Karlsruhe Institute of Technology for his thoughtful suggestions. This work was supported by the National Key R&D Program of China (2022YFB3204300), the National Natural Science Foundation of China (52103246), the Zhejiang Provincial Natural Science Foundation of China (LQ22E030015), the Natural Science Foundation of Ningbo (2023J408, 20221JCGY010301), the Ningbo International Cooperation Project (2023H019), and the Sino-German Mobility Program (M-0424).

Notes and references

1 R. Arppe and T. J. Sørensen, *Nat. Rev. Chem.*, 2017, **1**, 0031.
2 Y. Shen, X. Le, Y. Wu and T. Chen, *Chem. Soc. Rev.*, 2024, **53**, 606–623.
3 Y. Sun, X. Le, S. Zhou and T. Chen, *Adv. Mater.*, 2022, **34**, 2201262.
4 X. Wei, S. X. A. Zhang and L. Sheng, *Adv. Mater.*, 2022, **35**, 2208261.
5 X. Yu, H. Zhang and J. Yu, *Aggregate*, 2021, **2**, 20–34.
6 Y. Ai, Y. Fei, Z. Shu, Y. Zhu, J. Liu and Y. Li, *Chem. Eng. J.*, 2022, **450**, 138390.
7 H. Deng, H. Wang, Y. Tian, Z. Lin, J. Cui and J. Chen, *Mater. Horiz.*, 2023, **10**, 5256–5262.
8 L. Ding and X.-d Wang, *J. Am. Chem. Soc.*, 2020, **142**, 13558–13564.
9 G. Yin, G. Huo, M. Qi, D. Liu, L. Li, J. Zhou, X. Le, Y. Wang and T. Chen, *Adv. Funct. Mater.*, 2023, **34**, 2310043.
10 Y. Liu, D. Cheng, B. Wang, J. Yang, Y. Hao, J. Tan, Q. Li and S. Qu, *Adv. Mater.*, 2024, 2403775, DOI: 10.1002/adma.202403775.
11 Y. Sun, X. Le, H. Shang, Y. Shen, Y. Wu, Q. Liu, P. Théato and T. Chen, *Adv. Mater.*, 2024, **36**, 2401589.
12 W. C. Xu, C. Liu, S. Liang, D. Zhang, Y. Liu and S. Wu, *Adv. Mater.*, 2022, **34**, 2202150.
13 Y. Gao, K. Ge, Z. Zhang, Z. Li, S. Hu, H. Ji, M. Li and H. Feng, *Adv. Sci.*, 2024, **11**, 2305876.
14 Y. Zhao, X. Zhao, M. D. Li, Z. A. Li, H. Peng and X. Xie, *Angew. Chem., Int. Ed.*, 2020, **59**, 10066–10072.
15 Z.-H. Zuo, Z.-W. Feng, Y.-Y. Peng, Y. Su, Z.-Q. Liu, G. Li, Y. Yin and Y. Chen, *ACS Nano*, 2024, **18**, 4456–4466.
16 J.-H. Tian, H. Xu, X.-Y. Hu and D.-S. Guo, *Supramol. Mater.*, 2024, **3**, 100063.
17 L. Qin, X. Liu, K. He, G. Yu, H. Yuan, M. Xu, F. Li and Y. Yu, *Nat. Commun.*, 2021, **12**, 699.
18 J. Zhang, S. Qin, S. Zhang, C. Sun, Y. Ren, L. Zhang, J. Liu, J. Xiao, W. Hu, H. Yang and D. Yang, *Adv. Mater.*, 2023, 2305872, DOI: 10.1002/adma.202305872.
19 S. Chen, K. Zhang, Z. Li, Y. Wu, B. Zhu and J. Zhu, *Supramol. Mater.*, 2023, **2**, 100032.
20 M. Wu, L. Han, B. Yan and H. Zeng, *Supramol. Mater.*, 2023, **2**, 100045.
21 S. Lai, Y. Jin, L. Shi, R. Zhou and Y. Li, *ACS Appl. Mater. Interfaces*, 2022, **14**, 47113–47125.
22 D. Lou, Y. Sun, J. Li, Y. Zheng, Z. Zhou, J. Yang, C. Pan, Z. Zheng, X. Chen and W. Liu, *Angew. Chem., Int. Ed.*, 2022, **61**, e202117066.
23 H. Shang, X. Le, Y. Sun, S. Wu, Y. Wang, P. Théato and T. Chen, *Mater. Horiz.*, 2024, **11**, 2856–2864.
24 Q. Wang, Z. Qi, Q. M. Wang, M. Chen, B. Lin and D. H. Qu, *Adv. Funct. Mater.*, 2022, **32**, 2208865.
25 J. Xue, Y. Wang, T. Zhang, K. Li, F. Vogelbacher, Y. Zhang, X. Hou, Z. Zhu, Y. Tian, Y. Song and M. Li, *Sci. China: Chem.*, 2023, **66**, 3567–3575.
26 W. Zhao, B. Wu, Z. Lei and P. Wu, *Angew. Chem., Int. Ed.*, 2024, **63**, e202400531.
27 S. Wu, W. Li, Y. Sun, X. Zhang, J. Zhuang, H. Hu, B. Lei, C. Hu and Y. Liu, *J. Colloid Interface Sci.*, 2019, **555**, 607–614.
28 S. Deng, R. Deng, X. Mao, B. Xiong, M. Wang, S. Chen, W. H. Binder, J. Zhu and Z. Yang, *CCS Chem.*, 2023, **5**, 2301–2311.
29 P. H. Michels-Brito, V. Dudko, D. Wagner, P. Markus, G. Papastavrou, L. Michels, J. Breu and J. O. Fossum, *Sci. Adv.*, 2022, eabl8147.
30 Z. Zhang, Z. Chen, Y. Wang, Y. Zhao and L. Shang, *Adv. Funct. Mater.*, 2021, **32**, 2107242.

